Mutations in the Environment of the Primary Quinone Facilitate Proton Delivery to the Secondary Quinone in Bacterial Photosynthetic Reaction Centers†

Marie Valerio-Lepiniec,‡,§ Jaroslava Miksovska,‡,§ Marianne Schiffer,|| Deborah K. Hanson,|| and Pierre Sebban*,‡

Centre de Génétique Moléculaire, Centre National de la Recherche Scientifique, 91198, Gif/Yvette, France, and Center for Mechanistic Biology and Biotechnology, Argonne National Laboratory, 9700 South Cass Avenue, Argonne, Illinois 60439

Received March 3, 1998; Revised Manuscript Received September 16, 1998

ABSTRACT: In *Rhodobacter capsulatus*, we constructed a quadruple mutant that reversed a structural asymmetry that contributes to the functional asymmetry of the two quinone sites. In the photosynthetically incompetent quadruple mutant RQ, two acidic residues near Q_B, L212Glu and L213Asp, have been mutated to Ala; conversely, in the Q_A pocket, the symmetry-related residues M246Ala and M247Ala have been mutated to Glu and Asp. We have selected photocompetent phenotypic revertants (designated RQrev3 and RQrev4) that carry compensatory mutations in both the Q_A and Q_B pockets. Near Q_A, the M246Ala → Glu mutation remains in both revertants, but M247Asp is replaced by Tyr in RQrev3 and by Ala in RQrev4. The engineered L212Ala and L213Ala substitutions remain in the Q_B site of both revertants but are accompanied by an additional electrostatic-type mutation. To probe the respective influences of the mutations occurring near the Q_A and Q_B sites on electron and proton transfer, we have constructed two additional types of strains. First, "half" revertants were constructed that couple the Q_B site of the revertants with a wild-type Q_A site. Second, the Q_A sites of the two revertants were linked with the L212Glu-L213Asp → Ala-Ala mutations of the Q_B site. We have studied the electron and proton-transfer kinetics on the first and second flashes in reaction centers from these strains by flash-induced absorption spectroscopy. Our data demonstrate that substantial improvements of the proton-transfer capabilities occur in the strains carrying the M246Ala → Glu + M247Ala → Tyr mutations near Q_A. Interestingly, this is not observed when only the M246Ala → Glu mutation is present in the Q_A pocket. We suggest that the M247Ala → Tyr mutation in the Q_A pocket, or possibly the coupled M246Ala → Glu + M247Ala → Tyr mutations, accelerates the uptake and delivery of protons to the Q_B anions. The M247Tyr substitution may enable additional pathways for proton transfer that are located near Q_A.

Photosynthetic organisms convert light energy into chemical free energy. This conversion is achieved by photochemical reaction centers, which are embedded in the intracytoplasmic membrane of these organisms. The three-dimensional structures of these protein−pigment complexes have been determined for two different species of purple bacteria, *Rhodopseudomonas viridis (1)* and *Rhodobacter sphaeroides (2−7)*. The *Rb. sphaeroides* complex is about 100 kDa and is composed of three polypeptides. The L and M subunits are integral transmembrane proteins, but the H protein has only one transmembrane helix; its extrinsic domain essentially caps the reaction center at the cytoplasmic interface. All the pigments and cofactors present in the complex—four bacteriochlorophylls, two bacteriopheophytins (H_A and H_B), two quinone molecules (Q_A and Q_B), a non-heme iron atom, and a carotenoid molecule—are bound noncovalently to the L and M chains. Light absorption by the reaction center results in the excitation of a dimer of bacteriochlorophylls, P, to its lowest electronic singlet state, P*. In ∼200 ps, a transmembrane charge separation is stabilized between P^+, which is situated near the periplasmic side of the membrane, and Q_A^-, which is situated near the cytoplasmic side of the membrane. The electron present on Q_A is then transferred to the secondary quinone acceptor Q_B in 1−200 μs *(8−10)*. The binding sites for Q_A and Q_B share structural homology and are related by an axis of approximate 2-fold symmetry. Although both quinone acceptors are the same chemical species (ubiquinone$_{10}$) in *Rb. sphaeroides* and *Rhodobacter capsulatus*, they function in very different ways. Q_A, which is never directly protonated, functions as a one-electron acceptor. By contrast, after the successive absorption of two photons by the system, Q_B accepts two electrons and two protons from the cytoplasm to form the dihydroquinone Q_BH_2. This molecule, which is weakly bound to its site, leaves the reaction center and delivers its reducing power to the cytochrome bc_1 complex.

The presence of an extensive network of protonatable residues, which extends from the cytoplasm to the Q_B pocket, is an important and original feature of the reaction center structure *(4, 11−14)*. This web also involves many water molecules, as seen in the recent high-resolution reaction center structures *(4, 6, 15)*. Water molecules are also located in a cavity located near Q_A *(6, 14, 15)*. Structured and mobile water molecules have previously been suggested to participate in the proton-transfer process *(13, 15−20)*.

Studies of mutants from *Rb. sphaeroides* have suggested that L213Asp is directly involved in donation of the first

† Supported by Human Frontier of Science Organization Grant RG-329-95M, the Centre National de la Recherche Scientifique, and by the U.S. Department of Energy, Office of Biological and Environmental Research, under Contract W-31-109-ENG-38.

‡ CNRS.

§ The first two authors contributed equally to this work.

|| Argonne National Laboratory.

10.1021/bi980500t CCC: $18.00
Published on Web 12/16/1998

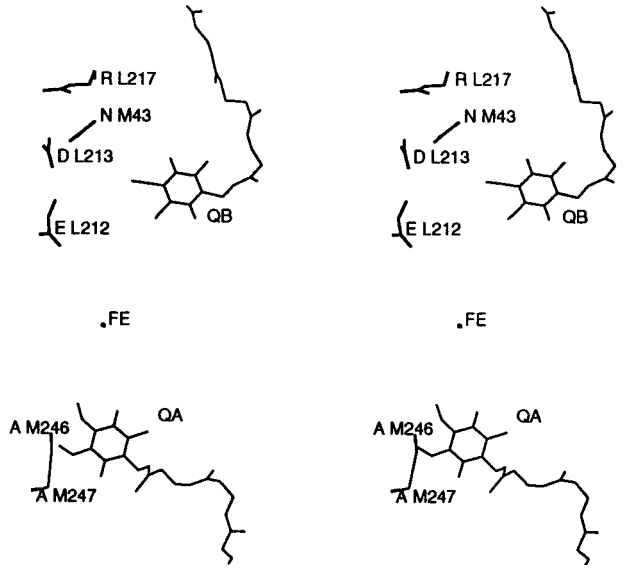

FIGURE 1: Stereoview based on the *Rb. sphaeroides* reaction center structure [dark structure *(6)*] showing the locations of the quinones and the amino acid residues described in the text and in Table 1. The wild-type residues are shown and are numbered according to the *Rb. capsulatus* sequence to correspond with the text. For clarity, the Cα atoms of the alanines at M246 and M247 were connected.

Table 1: Genotypes of Strains Included in This Study

	Q_B site				Q_A site		
strains	L212	L213	L217	M43	M246	M247	phenotype
wild type	Glu	Asp	Arg	Asn	Ala	Ala	PS^+
Site-Specific Mutants							
RQ	Ala	Ala			Glu	Asp	PS^-
AA	Ala	Ala					PS^-
RQ Phenotypic Revertants							
RQrev3	Ala	Ala		Asp	Glu	Tyr	PS^+
RQrev4	Ala	Ala	Cys		Glu		PS^+
Constructed Strains							
RQrev3B	Ala	Ala		Asp			PS^+
RQrev4B	Ala	Ala	Cys				PS^+
AA+3A	Ala	Ala			Glu	Tyr	PS^-
AA+4A	Ala	Ala			Glu		PS^-

proton to Q_B *(21, 22)*. L212Glu has been demonstrated to be an important component for transfer of the second proton to Q_B in *Rb. sphaeroides (23−26)* and in *Rb. capsulatus (20, 27)*. The symmetry-related counterparts of these residues in the Q_A binding pocket are nonprotonatable alanines (see Figure 1).

To probe the importance of this asymmetry in determining the functional properties of the quinones, we constructed a quadruple mutant of *Rb. capsulatus* in which residues L212Glu and L213Asp in the Q_B site and the symmetry-related residues M246Ala and M247Ala in the Q_A site are reversed. This mutant is designated RQ (L212Glu-L213Asp-M246Ala-M247Ala → Ala-Ala-Glu-Asp) *(28)*; it is unable to grow under photosynthetic conditions. Photocompetent phenotypic revertants (RQrev3 and RQrev4 strains; Table 1) have been isolated from this mutant that carry compensatory mutations in both the Q_A and the Q_B pockets. To track the relative influences of the Q_A- and Q_B-site mutations on the coupled electron−proton-transfer process, we have constructed two additional sets of strains. First, the Q_B- site mutations from the RQrev3 and RQrev4 revertants were coupled with a wild-type Q_A site (RQrev3B and RQrev4B strains, Table 1). Second, the Q_A-site mutations of the RQrev3 and RQrev4 strains were coupled with the L212Glu-L213Asp → Ala-Ala mutations (AA) in the Q_B site, yielding the AA+3A and AA+4A strains, respectively (Table 1). The photosynthetically incompetent AA double mutant has been characterized previously *(13, 16, 17, 29)*.

In this paper, we determine the rates of electron and proton transfer to Q_B following the first and second flashes in the reaction centers from these strains. By comparing the effects of the mutations in the Q_A site, we show that the M246Ala → Glu + M247Ala → Tyr mutations near Q_A lead to a notable improvement in the ability of these reaction centers to transfer protons to the Q_B site. This is not the case when only the M246Ala → Glu mutation is present. In addition, our data show that, after the first flash, fast electron transfer precedes very slow protonation events in the severely impaired mutants. After the second flash, the transfer of the second electron is rate-limited by the slowest proton uptake kinetics.

MATERIALS AND METHODS

Bacterial Strains and Culture. The construction of the RQ quadruple mutant, in which the sequence asymmetries present at the L212Glu-L213Asp vs M246Ala-M247Ala sites are reversed, and the description of the isolation and genotypic characterization of spontaneous phenotypic revertants has been described *(28)*. The construction of the L212Glu-L213Asp → Ala-Ala double mutant (AA) has been reported previously *(17, 30)*. The genotypes of the strains used in the present study are listed in Table 1. Since the RQ revertants carry compensatory mutations in both the L and M genes, unique restriction sites in plasmids pU29 *(31)* and pU2922 *(32)* were used to construct the RQrev3B and RQrev4B "half" revertants. These strains carry a wild-type Q_A site coupled to a Q_B site that was derived from the particular phenotypic revertant. The AA+3A and AA+4A mutants were constructed following the same procedure; they couple the AA mutations in the Q_B site with the Q_A site that is derived from the particular revertant. The RQrev3B and RQrev4B strains were able to grow under photosynthetic conditions (PS^+); the AA+3A and AA+4A strains are photosynthetically incompetent (PS^-).

For reaction center preparations, cells were grown semi-aerobically in the dark (34 °C) in RPYE medium *(16)*. Purification of reaction centers has been described previously *(33)*.

Spectroscopic Measurements. The $P^+Q_A^-$ and $P^+Q_B^-$ charge recombination kinetics were followed at 865 nm on a homemade spectrophotometer *(27)*. The $P^+Q_B^-$ charge recombination kinetics were measured in the presence of excess quinone [1−2 μM RCs; ∼50−75 μM UQ_6 (Sigma)]. In the strains carrying Q_A-site mutations, a large fraction of the bound Q_A was lost after the detergent purification of reaction centers. Upon the addition of exogenous quinone, reconstitution of the Q_A site was monitored by measuring the amplitude of the $P^+Q_A^-$ charge recombination signal. In the strains with mutant Q_A sites, the affinity for Q_A was reduced compared to the wild type [∼0.1 μM^{-1} *(34)*], but more than 80% of native Q_A activity was restored upon addition of ∼1 μM UQ_6. In these reaction centers, and in

the presence of a large excess of exogenous quinone, Q_A^- was found to be rapidly reoxidized (≤100 ms), probably because of electron donation to the external quinone pool. Under these conditions, addition of terbutryn resulted in the formation of a slowly decaying P^+ state in about 50−60% of the reaction center population. Thus, in these reaction centers, the $P^+Q_A^-$ charge recombination kinetics were measured in the presence of a very small amount of UQ_6 (∼1−2 μM) in order to selectively reconstitute the Q_A binding site. The rates for transfer of first electron were measured at 750 nm, in the electrochromic band shift of the bacteriopheophytin *(9)*. The rates of transfer of a second electron were measured at 450 nm, monitoring the disappearance of the $Q_A^-Q_B^-$ state *(35, 36)*. These measurements were made in the presence of 40 μM cytochrome *c*, 200−500 μM ascorbic acid, and 50−75 μM UQ_6. The multiflash cytochrome oxidation experiments were done at 550 nm, in the presence of 20−40 μM cytochrome *c* reduced by 250−500 μM ascorbic acid, 50−75 μM UQ_6, and 1 μM RC.

Buffers (10 mM) used were as follows: 2-(*N*-morpholino)-ethanesulfonic acid (MES; Sigma) between pH 5.5 and 6.5; 1,3-bis[tris(hydroxymethyl)methylamino]propane (Bis-tris propane; Sigma) between pH 6.3 and 9.5; and 3-(cyclohexylamino)propanesulfonic acid (CAPS; Calbiochem) above pH 9.5.

Proton-Transfer Measurements. The kinetics of proton uptake were determined at pH 7.5 by measuring the absorbance changes at 580 nm (isosbestic point of the P^+ absorbance changes) of the pH-sensitive dye *o*-cresol red. The assay solution contained 1−2 μM reaction centers, 50 mM NaCl, 0.03% Triton X-100, 100 μM ferrocene, 500 μM potassium ferrocyanide, 60 μM UQ_6, and 40 μM *o*-cresol red. The reaction centers were extensively dialyzed in order to keep the buffer concentration below 5−10 μM. The absolute calibrations of the stoichiometries of proton uptake were performed by additions of known amounts of HCl (1 M stock; Merck) as previously described *(27)*. The net proton uptake (H^+/Q_B^-) was obtained by subtracting the buffered signal from the unbuffered signal. The occupancy of the Q_B binding pocket was calculated from the ratio of cytochrome *c* oxidation after the second flash to that after the first flash (measured at 550 nm), and from the relative amount of the slow phase of charge recombination ($P^+Q_B^-$, measured at 865 nm).

In the AA, AA+3A, and AA+4A strains, the $P^+Q_B^-$ charge recombination process was found to be very slow (≅ 0.08−0.1 s^{-1} at pH 7.5) suggesting a very stable Q_B^- state. Therefore, special care was taken in the double-flash proton uptake kinetics, cytochrome oxidation turnover, and second electron transfer measurements to thoroughly dark-adapt the samples. The samples were held for more than 1 h in the dark before illumination. Also, we verified that the addition of a few micromolar of potassium ferricyanide (to reoxidize any residual Q_B^- state) did not increase the amplitude of the flash-induced $P^+Q_B^-$ signal.

RESULTS

Compensatory Mutations in the Phenotypic Revertants. The mutations carried by the two phenotypic revertants and the constructed mutants are summarized in Table 1. From the PS^- RQ mutant, the photocompetent RQrev3 and RQrev4 phenotypic revertants were selected. Both phenotypic revertants carry the L212Ala-L213Ala mutations in the Q_B pocket and the single additional mutation M43Asn → Asp (∼9 Å from Q_B) or L217Arg → Cys (∼11 Å from Q_B), respectively. At the Q_A site, the engineered M246Ala → Glu mutation remains in both phenotypic revertants, but the engineered Asp at position M247 is replaced. In RQrev3, Tyr replaces Asp, whereas in the RQrev4 strain, the wild-type Ala was restored by a genotypic reversion. The M247Asp → Tyr mutation is also present in another independent phenotypic revertant that we have selected from the RQ mutant, suggesting that the presence of Tyr in position M247 is of importance in restoring the function lost in the RQ mutant *(28)*. The functional capabilities of this other phenotypic revertant are very similar to those of the RQrev3 strain presented here (unpublished observations).

Table 2: Rates of $P^+Q_A^-$ and $P^+Q_B^-$ Charge Recombination and Second Electron Transfer Reactions[a] Measured at pH 7.5

strain	k_{AP} (s^{-1})	k_{BP} (s^{-1})	$k_{AB}(2)$ (s^{-1})
wild type	7.8 ± 0.3	0.83 ± 0.05	2500 ± 200
Site-Specific Mutants			
RQ	6.3 ± 0.3	0.05 ± 0.01	1.5 ± 0.2
AA	7.6 ± 0.3	0.08 ± 0.01	0.5 ± 0.1
RQ Phenotypic Revertants			
RQrev3	7.8 ± 0.3	0.09 ± 0.01	30 ± 3
RQrev4	8.2 ± 0.3	0.90 ± 0.05	1.5 ± 0.2
Constructed Strains			
RQrev3B	8.1 ± 0.3	0.17 ± 0.08	5 ± 0.3
RQrev4B	7.0 ± 0.3	0.85 ± 0.02	3.3 ± 0.5
AA+3A	6.9 ± 0.3	0.08 ± 0.01	3.5 ± 0.5
AA+4A	6.6 ± 0.3	0.10 ± 0.01	0.8 ± 0.1

[a] For conditions, see Materials and Methods.

$P^+Q_B^-$ Charge Recombination Rates. The rates of the $P^+Q_B^-$ charge recombination (k_{BP}) in the reaction centers of the various strains are presented in Table 2. We have measured these rates over the pH range 6−11 (data not shown). Because k_{BP} is nearly pH-independent in the neutral pH range in all the strains, we list only the values for k_{BP} obtained at pH 7.5. The rates of the $P^+Q_A^-$ charge recombination (k_{AP}) were also measured in all strains studied here (Table 2). They do not vary more than ∼20% with that of the wild type. Therefore, changes in the k_{BP} values reflect changes in the $Q_A^-Q_B \leftrightarrow Q_AQ_B^-$ apparent equilibrium constant [$K_2 = (k_{AP}/k_{BP}) - 1$] *(37)*. The k_{BP} values measured in the RQrev4 and RQrev4B strains are nearly the same ($k_{BP} \approx 0.9$ and 0.85 s^{-1}, respectively) and are substantially increased compared to the reaction centers from the AA mutant ($k_{BP} = 0.08$ s^{-1}). We have already pointed out the significant electrostatic effect of the L217Arg → Cys mutation in the RQrev4 reaction center *(38)*. This mutation increases k_{BP} about (and decreases K_2 by) the same value at pH 7.5 as compared to the value in the AA reaction center. This leads to a decrease in the free energy gap between the $P^+Q_B^-$ and $P^+Q_A^-$ states in the RQrev4 reaction center of at least 75 meV. The M43Asn → Asp mutation present in the RQrev3B reaction center does not produce such a dramatic effect. k_{BP} in this reaction center (0.17 s^{-1}) is increased by only a factor of 2 when compared to that of the AA mutant. k_{BP} is somewhat decreased in the RQrev3 reaction center (0.09 s^{-1}) as compared to that of RQrev3B.

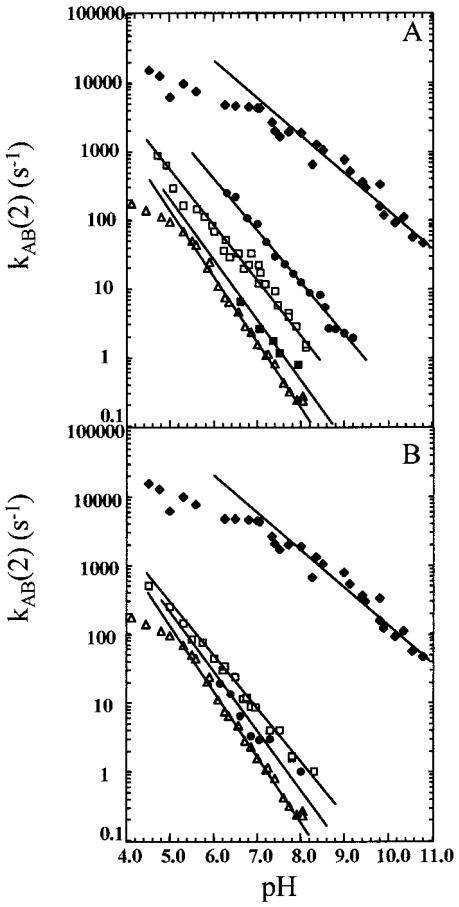

FIGURE 2: pH dependence of the rate constant of the second electron-transfer reaction from Q_A^- to Q_B^-, measured at 450 nm in reaction centers (~2 μM) from the following strains: (A) RQrev3 (●), RQrev3B (□), RQ (■), AA (△), and the wild type (◆); (B), RQrev4 (●), RQrev4B (□), AA (△), and the wild type (◆). Conditions: 0.05% LDAO or 0.03% Triton X-100, buffers depending on pH as indicated in the text, 50−75 μM UQ_6, 21 °C, 40 μM cytochrome *c*, and 200−500 μM sodium ascorbate.

Rate Constant for the Second Electron-Transfer Reaction, $k_{AB}(2)$. The pH dependencies of the rate constant for the second electron-transfer reaction, $k_{AB}(2)$, measured in the reaction centers from the RQ, RQrev3B, RQrev3, AA, and wild-type strains are presented in Figure 2A. We have also measured $k_{AB}(2)$ in the AA+3A and AA+4A strains at pH 7.5 (Table 2).

The pH dependencies of $k_{AB}(2)$ for the wild type and the AA mutant have previously been measured *(29)*. In the pH range 6.5−8.0, $k_{AB}(2)$ in the RQ mutant is slightly greater than in the AA mutant. At pH 7.5, $k_{AB}(2)$ for the RQ mutant is about 1.5 s^{-1} versus 0.5 s^{-1} for the AA mutant. The $k_{AB}(2)$ values measured at pH 7.5 for the AA family are shown in Table 2. In the AA+4A reaction center, $k_{AB}(2)$ is very slightly increased (0.8 s^{-1}) compared to that of the AA mutant. In the AA+3A reaction center, $k_{AB}(2)$ is more notably increased to a value of 3.5 s^{-1}. $k_{AB}(2)$ values of the RQrev3B mutant are about 3−4 times greater than those measured in the RQ mutant. Interestingly, in the whole pH range studied, the $k_{AB}(2)$ values in the RQrev3 strain are notably higher than those of the RQrev3B strain. At pH 7.5, $k_{AB}(2)$ is accelerated approximately 6-fold in the reaction centers of the RQrev3 strain [$k_{AB}(2) \cong 30$ s^{-1}] compared to those of RQrev3B (5 s^{-1}), even though these two strains have the same protein sequence in the Q_B pocket. This suggests the involvement of the mutations present in the Q_A pocket of the RQrev3 strain in modifying this rate.

The slope of the pH dependence of $k_{AB}(2)$ provides some information about the specificity of the diffusion of protons in the protein. A slope of −1 H^+/e^- indicates a diffusion-limited process for proton transfer. A slope that is less negative reflects a protein-limited process. In the wild-type reaction centers, this slope is about −0.63 H^+/e^- above the apparent pK_a of about 8.2. For all other strains, a more negative slope is observed, suggesting that the transfer of protons may occur by less specific pathways than in the wild type. In the pH range 6−8, the reaction centers of the RQrev3 strain display a slope similar to that of the RQrev3B reaction centers (~−0.75 H^+/e^-). In the RQ mutant, this value is about −0.70 H^+/e^-. In the AA mutant, this slope is ~ −0.80 H^+/e^-.

The pH dependencies of the $k_{AB}(2)$ values for the RQrev4 and RQrev4B reaction centers are presented in Figure 2B and are compared with the data obtained for the AA mutant and the wild type. In the pH range 6−8, the $k_{AB}(2)$ values for the RQrev4B mutant are 3−7 times higher than those of the AA reaction centers. At pH 7.5, $k_{AB}(2)$ is about 3.3 s^{-1} in the RQrev4B reaction center. In contrast to the situation with the RQrev3 family, no improvement of the second electron-transfer capabilities is detected in the RQrev4 reaction center as compared to that of the RQrev4B strain. The data from the RQrev4 and RQrev4B reaction centers display slopes of about −0.70 and −0.72 H^+/e^-, respectively. Note that these strains are photocompetent whereas the RQ mutant, which is characterized by similar $k_{AB}(2)$ values, is not. Thus, the second electron-transfer step is not the limiting one for photosynthetic growth in the RQ mutant (see Discussion).

Multiflash Cytochrome Photooxidation. To characterize the functional behavior of the reaction centers of the various strains further, we have measured their patterns of cytochrome photooxidation after several flashes. These data provide information about the photocycling time of the reaction centers. The measurements were made at 550 nm, pH 7.5, in the presence of reduced cytochrome *c*. The data were normalized to the amplitude of cytochrome oxidation on the first flash. In the data presented here, the flash spacing is 100 ms. Patterns of cytochrome photooxidation for reaction centers of the wild type, RQrev3, and RQrev3B are presented in Figure 3 (upper panel). The pattern for the RQrev3B reaction centers displays a progressive damping of the amplitudes of the oxidation steps after the third flash. This reflects the inability of the reaction centers from this strain to achieve photochemical cycling within 100 ms. The wild-type and, interestingly, the RQrev3 reaction centers are fully capable of completing a cycle during each 100 ms interval (data nearly superimposable).

The cytochrome oxidation patterns for the reaction centers of the AA, AA+3A and AA+4A strains are presented in Figure 3 (lower panel). A substantial damping of the oxidation steps after the second and third flashes is displayed for the reaction centers from the AA and AA+4A strains. In the AA mutant, we previously attributed this behavior to the inability of the reaction centers to form the Q_BH_2 state in the interval between the second and the third flashes (100 ms), due to the severe impairment of its proton-transfer capabilities *(16)*. The situation is different for the AA+3A

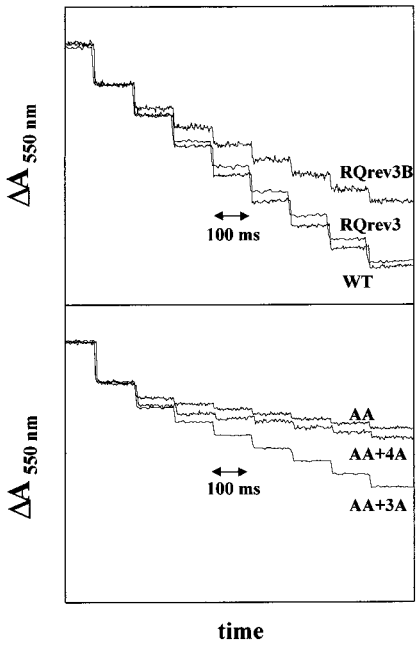

FIGURE 3: Multiflash cytochrome *c* oxidation in reaction centers (~1 μM) from the following strains: (upper panel) RQrev3, RQrev3B, and the wild type and (lower panel) AA, AA+4A, and AA+3A. The curves are normalized to the amplitude of the oxidation step measured after the first flash. Conditions: 10 mM Tris, pH 7.8, LDAO 0.05%, 40 μM cytochrome *c*, 250−500 μM sodium ascorbate, 50−75 μM UQ_6; 550 nm.

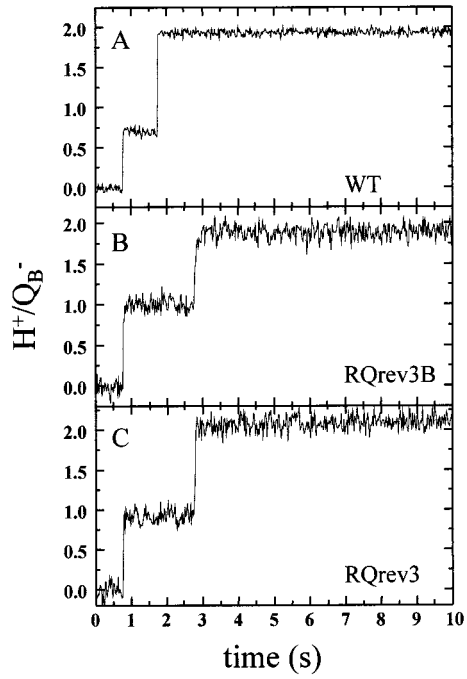

FIGURE 4: Stoichiometries and kinetics of proton uptake after the first and second flashes in reaction centers (~1−2 μM) from the wild-type, RQrev3B, and RQrev3 strains. Conditions: 50 mM NaCl, 0.03% Triton X-100, pH 7.5, 100 μM ferrocene, 500 μM potassium ferrocyanide, 60 μM UQ_6, 40 μM *o*-cresol red; 580 nm. The net proton uptake was obtained by subtracting the buffered signal from the unbuffered traces.

reaction centers, where a slight damping exists after the third flash but the amplitude of the cytochrome oxidation remains nearly the same on the following flashes. This reflects the ability of the reaction centers from this strain to function quasi-normally at a flash repetition rate of 10 Hz. These data demonstrate a significant improvement in the function of the RQrev3 and AA+3A reaction centers, which carry the M246Glu-M247Tyr mutations near Q_A, as compared to the RQrev3B and AA reaction centers, which do not. However, it is clear that the M246Glu mutation is not responsible for the observed effect because no improvement in cytochrome oxidation rates is seen for the AA+4A reaction center that carries the M246Ala → Glu mutation but does not have the Tyr substitution at M247.

Kinetics of Proton Uptake after the First and Second Flashes. The kinetics of proton uptake measured after two flashes for the reaction centers of the wild-type, RQrev3B, and RQrev3 strains are presented in Figure 4. These data were obtained at pH 7.5, in the presence of the pH indicator *o*-cresol red. In the wild type (Figure 4A), about 0.70 ± 0.05 H^+/Q_B^- are rapidly (<1 ms) taken up on the first flash. Such partial stoichiometry has previously been attributed to proton uptake by residues whose pK_as are shifted upon reduction of Q_B *(39, 40)*. On the second flash, uptake complementary to 2 H^+/Q_B^- is observed on a fast time scale. These data for the wild-type *Rb. capsulatus* reaction center were reported previously *(20, 27)*. The situation is slightly different for the RQrev3B reaction center (Figure 4B). About 1.00 ± 0.05 H^+/Q_B^- is taken up on the first flash. This larger amplitude of proton uptake measured on the first flash, relative to the wild type, has been reported previously for the L213DN reaction center mutant from *Rb. sphaeroides (22, 41)*. A small fraction (≈ 5−10%) of the proton uptake observed in the RQrev3B reaction centers on the first flash occurs on a slower time scale (≈100 ms). On the second flash, uptake complementary to $2H^+/Q_B$ occurs. Most of the kinetics observed on the second flash are fast (≤20 ms), but about 20% of the uptake occurs with a rate of about 120 ms (Table 3).

Table 3: Proton Uptake Lifetimes[a] Measured after the Second Flash, pH 7.5

	fast phase		slow phase	
strain	amplitude (%)	$1/k_H^+$ (ms)	amplitude (%)	$1/k_H^+$ (s)
wild type	100	≤1		
RQrev3	100	≤20		
RQrev3B	~80	≤20	~20%	0.12 ± 0.03
AA	~20	≤20	~80	0.80 ± 0.08
AA+3A	≥50	≤20	≤50	0.18 ± 0.02
AA+4A	~20%	≤20	~80	0.80 ± 0.08

[a] Conditions were as in Figures 4 and 5.

In the reaction centers from the RQrev3 strain, 0.90 ± 0.05 H^+/Q_B^- is taken up on the first flash (Figure 4C). Compared to the RQrev3B strain, the RQrev3 reaction centers carry the additional M246Glu-M247Tyr mutations near Q_A (Table 1), and the proton uptake occurs rapidly on both the first and second flashes, giving rise to a nearly native pattern of proton uptake kinetics on the time scale of Figure 4C. [On the second flash, the slowest phase of proton uptake in the RQrev3 reaction centers is ≤20 ms (data not shown).]

The kinetics of proton uptake measured in the reaction centers of the AA, AA+4A, and AA+3A mutants are presented in Figure 5. In these three strains, at pH 7.5, the amplitude of proton uptake on the first flash is 1.00 ± 0.20 H^+/Q_B^- and is nearly 2 H^+/Q_B after two flashes. In the AA

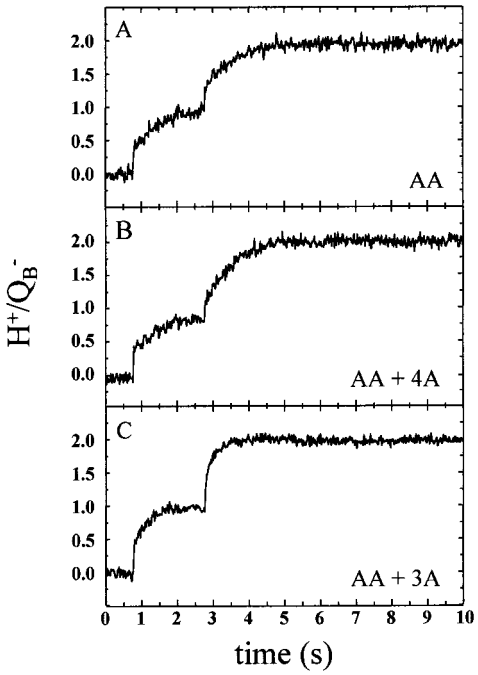

FIGURE 5: Stoichiometries and kinetics of proton uptake after the first and second flashes in reaction centers (~1−2 μM) from the AA, AA+4A, and AA+3A strains. Conditions were as for Figure 4.

mutant (Figure 5A), the first flash induces strongly biphasic kinetics of proton uptake. The fast phase, which represents about 0.35 H^+/Q_B^-, has a time constant of several milliseconds (data not shown). The slow phase, which accounts for about 0.65 H^+/Q_B^-, has a time constant of about 0.85 s. On the second flash, the same overall kinetic behavior is observed. In the AA+4A reaction centers, no improvement of the proton-transfer capabilities is observed as a result of the additional M246Ala → Glu mutation. On the first flash, proton uptake occurs in a biphasic process with time constants similar to those of the AA mutant reaction center. On the second flash, only 20% of the proton uptake is fast [whereas 80% of the signal has a time constant of ~0.80 s (Table 3)].

The AA+3A mutant (Figure 5C) is significantly more capable of performing proton transfer compared to the AA or AA+4A strains. First, the relative amplitudes of the fastest (≤20 ms) phases are increased to ~50% and ≥50%, respectively, of the total proton uptake on both the first and second flashes. In addition, the slow phases are accelerated when compared to those of the AA and AA+4A reaction centers. On the first flash, the slow phase has a time constant of about 0.25 s (versus 0.85 s seen for the AA and AA+4A reaction centers). The acceleration is even greater on the second flash (~ 0.18 s, versus 0.80 s for AA or AA+4A) (Table 3). This correlates with the overall improvement in the function of the AA+3A reaction center, which was evident from the cytochrome photooxidation measurements (Figure 3B).

Kinetics of Transfer of the First Electron from Q_A^- to Q_B. We have measured the kinetics of transfer of the first electron from Q_A^- to Q_B in order to determine whether the slow protonation events influence the electron-transfer reaction. The rate constants measured at 750 nm, pH 7.5, are presented in Table 4. Except for the RQrev3B and AA+4A strains, the kinetics are exponential. In the wild type, the time constant for the $Q_A^- \rightarrow Q_B$ electron-transfer reaction is about 85 μs. In the wild-type *Rb. sphaeroides* reaction centers, more complex kinetics have been reported, including the presence of 30−40 μs and 220−250 μs phases *(9, 10)*. The presence of a faster component (≈1 μs) with a very small amplitude has been proposed recently *(10)*. Within the resolution of our instrument (a few microseconds), we do not observe heterogeneity of the "fast" phase (<100 μs) in the reaction center of any strain described here.

Table 4: Kinetics of Transfer of the First Electron[a] from Q_A^- to Q_B, pH 7.5, 750 nm

	$1/k_{AB}(1)$ (μs)	
strain	fast	slow
WT	85 ± 10	
RQ	55 ± 10	
RQrev3	88 ± 10	
RQrev3B	84 ± 10 (66%)	2900 ± 300 (33%)
AA	100 ± 10	
AA+3A	87 ± 10	
AA+4A	108 ± 10 (60%)	3200 ± 300 (40%)

[a] For conditions, see Materials and Methods.

Despite the differences in their k_{BP} values (i.e., the $Q_A^-Q_B \leftrightarrow Q_AQ_B^-$ equilibrium constants; Table 2), the lifetimes of the fast components of the first electron-transfer reactions do not vary more than 2-fold in the reaction centers of all of the strains studied. As described above for proton uptake, the kinetics measured in reaction centers from the RQrev3B and AA+4A strains show notable biphasicity. In addition to the fast phase, a ~3 ms component with an amplitude of ~33% or ~40%, respectively, has also been detected. We have also measured the kinetics of all these strains at 770 nm (data not shown). It has been suggested that the absorbance changes detected at this wavelength may reflect protonation events triggered by or associated with electron transfer from Q_A^- to Q_B *(9)*. At room temperature, no significant differences could be detected between the data measured at 770 nm vs 750 nm.

DISCUSSION

To probe the asymmetry in the reaction center quinone sites that pertains to the L212Glu-L213Asp versus M246Ala-M247Ala pairs of residues, we initially constructed the quadruple mutant RQ (L212Glu-L213Asp-M246Ala-M247Ala → Ala-Ala-Glu-Asp). L213Asp and L212Glu have been shown to be involved in the rapid delivery of the first and second protons, respectively, to Q_B *(21, 26)*. When L212Glu and L213Asp are mutated to Ala, the mutant strain is incapable of photosynthetic growth because proton delivery to the Q_B anions is impaired *(13, 16, 17, 20, 29)*. The substitution of M246Ala and M247Ala by acidic residues also yields a PS^- strain *(30)*; reaction centers of the M246Glu-M247Asp mutant are characterized by reduced binding of Q_A and a 10-fold reduction in the rate of $H_A \rightarrow Q_A$ electron transfer (P. D. Laible and D. K. Hanson, unpublished observations). The two phenotypic revertants of the RQ strain that are studied here (RQrev3 and RQrev4) carry changes in both the Q_A and Q_B sites. One of our main goals was to determine whether the mutations in the Q_A site assist in the delivery of electrons and/or protons to Q_B. To

this end, we have separated the Q_A- and Q_B-site mutations from each other by constructing "half-revertant" reaction centers (RQrev3B and RQrev4B strains; Table 1). We have also combined the mutant Q_A sites found in RQrev3 and RQrev4 with the L212Ala-L213Ala mutant Q_B site (AA+3A and AA+4A strains; Table 1). This is the first report that describes the effects of distant mutations near Q_A on proton transfer to Q_B.

Our data show that the functional capacities of proton uptake and delivery to Q_B are strikingly improved in reaction centers carrying the M246Ala → Glu + M247Ala → Tyr mutations near Q_A (RQrev3 and AA+3A strains). No improvement is observed in reaction centers where only the M246Ala → Glu mutation is present (RQrev4 and AA+4A strains).

In the RQrev3 reaction center, $k_{AB}(2)$ is increased about 6-fold compared to that of RQrev3B. This is not observed for the RQrev4 reaction center, which has a $k_{AB}(2)$ value that is 50% slower than that of the RQrev4B strain (Table 2). It was shown previously that the M43Asn → Asp mutation near Q_B (present in RQrev3 and RQrev3B) is very efficient in restoring rapid rates of proton transfer and second electron transfer to reaction centers that lack either L212Glu *(*20*)* or L213Asp *(42)*. Therefore, the further acceleration of these processes that is seen when the M246Glu and M247Tyr substitutions are added in the RQrev3 reaction center is surprising. This trend is confirmed by the patterns of cytochrome oxidation after multiple flashes (Figure 3). When the flash spacing is 100 ms, the reaction centers from the RQrev3 strain display nearly native behavior in contrast to the reaction center of RQrev3B, in which oxidation steps are progressively damped with successive flashes. The AA+3A mutant shows quasi-normal steps of cytochrome oxidation while the AA+4A mutant does not. The absence of the effect in the RQrev4 and AA+4A reaction centers rules out a major role for the single M246Glu mutation in the acceleration of proton transfer and second electron-transfer reactions.

Proton and Electron Transfer on the First Flash. In isolated reaction centers, the partial proton uptake observed on the first flash is due to pK_a shifts induced by the formation of Q_B^- *(39, 40)*. In the reaction centers of the wild type, RQrev3, and RQrev3B, rapid monophasic kinetics are measured (Figure 4). In contrast, the strains that are more seriously impaired show biphasic kinetics (Figure 5). The fast phase of proton uptake is likely to arise from the transfer of protons from the bulk phase to proteic groups that are distant from the L212 and L213 positions; these peripheral groups are therefore not influenced by the absence of L212Glu and L213Asp. The proton-transfer kinetics to peripheral groups should occur with rates comparable to those measured in the wild type (≤ milliseconds). The slow phase of proton uptake detected in the AA (≈0.85 s), AA+4A (≈0.85 s), and AA+3A (≈0.25 s) reaction centers may reflect proton uptake by groups that are influenced by L212Glu and L213Asp and are more significantly affected by their substitution with neutral residues. In the wild type, the residues involved in these phenomena probably interact with L212Glu and L213Asp directly or interact with them indirectly via a web of hydrogen-bonded residues and water molecules. Therefore, on the first flash, the amplitude of the slow phase of proton uptake in reaction centers carrying the AA mutations should be roughly comparable to the fraction of proton uptake in the wild type that can be assigned to the putative groups which interact strongly with L212Glu and L213Asp.

Proton uptake with the first flash is substantially slowed in the AA mutant. In the AA+3A reaction center, an appreciable acceleration of the kinetics of proton transfer is observed on the first flash compared to the AA mutant (Figure 5). The amplitude of the slow phase decreased from 65% (AA) to 50% (AA+3A), and the lifetime of this phase decreased from 0.85 s (AA) to 0.25 s (AA+3A). This is not seen in the AA+4A reaction center, which displays kinetics that are very similar to those of the AA mutant.

The rapid proton uptake with both the first and second flashes that we have measured in the RQrev3B and RQrev3 strains (which carry the AA and M43Asn → Asp mutations in the Q_B site) demonstrates the remarkable ability of M43Asp to assume the roles of both L212Glu and L213Asp. This suggested that similar pathways and processes could be involved for proton transfers on both the first and second flashes *(20)*.

In all strains, the kinetics for the first electron transfer measured at 750 nm are fast (≤100 μs), except for a slow component of about 3 ms in the RQrev3B and AA+4A strains. The fast phase is likely to originate from electron transfer before reorganization of the protein *(9)*. The slow phase of electron transfer was previously suggested to arise from electron-transfer rate-limited by rearrangement of the protein *(10)*. In the reaction centers carrying the AA mutations where the first-flash protonation steps are slow, electron transfer occurs at a rate similar to that of the wild type. Therefore, the very slow phases of proton uptake (>100 ms) reflect protonation events occurring long after electron transfer is completed. These observations show that, at least in these mutants, electron transfer on the first flash is not rate-limited by the process of partial proton uptake near Q_B.

In the modified strains that carry the AA mutations, the amplitude of proton uptake on the first flash (pH 7.5) ranges between 0.85 ± 0.05 and 1.00 ± 0.05 H^+/Q_B^-. This amplitude is systematically greater than the amount of proton uptake that is observed for the wild-type reaction center at the same pH (≈0.72 ± 0.05 H^+/Q_B^-). Experimental data obtained in *Rb. capsulatus (27)* and *Rb. sphaeroides* reaction centers *(43, 44)* as well as electrostatic calculations (*45*; E. Alexov and M. R. Gunner, personal communication), have suggested that L212Glu is mostly protonated at neutral pH. The replacement of Glu by Ala, therefore, is not expected to cause a significant change in the protonation state of the reaction centers at pH 7.5. However, the replacement of L213Asp, which is ionized at pH 7.5 *(21, 22, 24)*, by Ala would be expected to cause shifts in the pK_as of some of the residues interacting with Q_B. The shift of high pK_as (e.g., >7.5 in the wild type*)* closer to 7.5 would allow those residues to participate in partial proton uptake in the modified strains studied here. The pK_as of acidic residues that closely interact with L213Asp would also be expected to shift to lower values in its absence. Residues L210Asp and H173Glu, which were suggested to interact strongly with L213Asp (E. Alexov and M. R. Gunner, personal communication), are likely to be involved in the increased H^+/Q_B^- values measured here in the modified strains.

Proton and Electron Transfer on the Second Flash. In contrast to what is observed on the first flash, where slow protonation steps follow fast electron transfer, the second electron transfer rates are limited by the slowest proton uptake events. This is true even when the slow phase of proton uptake represents only a small fraction of the kinetics measured on the second flash. For example, in the RQrev3B strain at pH 7.5, $k_{AB}(2) \cong 5\ s^{-1}$, and the slow phase of the proton uptake (amplitude of ~20%) has a time constant of about 120 ms. Also, in the AA mutant, the slow proton uptake kinetics (~0.80 s; ~80% of the total) match, within a factor of 2, the $k_{AB}(2)$ value measured at pH 7.5 ($0.5\ s^{-1}$) Takahashi et al. *(41)* and Paddock et al. *(22)* have observed similar behavior for the L213DN mutant from *Rb. sphaeroides*. These authors measured rates of secondary electron transfer processes roughly matching the rate of the slow phase of proton uptake on the second flash. This is consistent with our data and suggests that, in the mutants that are impaired in proton transfer, the slow phase of proton uptake on the second flash approximately corresponds to the limiting kinetic step for transfer of the second electron to Q_B.

In the L212Glu → Gln mutant from *Rb. sphaeroides (23)* or *Rb. capsulatus (27)*, in which the delivery of only the second proton is slow, the $k_{AB}(2)$ values are essentially the same as that of the wild type. When Ala replaces Gln in position L212, the reaction centers recover their ability to deliver the second proton at a rate close to the wild type *(27)*. Our present data obtained in strains carrying Ala in position L212 confirm that the kinetic process coupled with the slow second electron transfer is related to the transfer of the first proton.

The improvements of the proton-transfer capabilities that were seen on the first flash in strains containing the M246Ala → Glu and M247Ala → Tyr mutations are displayed even more clearly on the second flash. The acceleration of the kinetics of proton transfer in the reaction centers of RQrev3, as compared to RQrev3B, and AA+3A, as compared to AA or AA+4A, affects not only the lifetime of the slow (> 100 ms) phase but also the relative amplitude of this phase. The slow phase of proton uptake ($\tau \sim 120$ ms) that is present on the second flash in the RQrev3B reaction center (Figure 4) accelerates so greatly in the RQrev3 reaction center ($\tau \leq 30$ ms; see Results) that it is not observable in the time window of Figure 4. Similarly, in the AA+3A reaction centers, the slow phase of proton uptake represents less than 50% of the total proton uptake measured on the second flash. It is significantly accelerated to ~0.18 s, compared to what is measured for the AA and AA+4A reaction centers (~0.80 s; 80% amplitude).

Our data emphasize the acceleration of the proton transfer process that occurs in the reaction centers from the RQrev3 and AA+3A strains, respectively, compared to the RQrev3B and AA strains. Indeed, in impaired reaction centers like those carrying the AA mutations, it is likely that the changes in the proton-coupled electron transfer rates measured on the second flash can be attributed to modifications in the efficiency of proton transfer. These reaction centers behave very similarly to those of the L213Asp → Asn mutant from *Rb. sphaeroides*, in which transfer of the second electron was shown to be proton-limited *(46)*. As mentioned above, the L212Glu → Ala mutation of *Rb. capsulatus* does not impair reaction center function significantly since the L212Ala single mutant grows photosynthetically and displays nearly wild-type proton-transfer kinetics *(27)*. Thus, in the AA mutant, the L213Asp → Ala mutation is responsible for limiting the capabilities of the AA reaction center in the same way that the L213Asn mutation does in the *Rb. sphaeroides* reaction center. In the RQrev3B reaction centers, the slow (~120 ms) fraction of the proton uptake kinetics on the second flash is very likely to represent the proton-limited portion of the kinetics. Indeed, in the RQrev3 reaction centers, this phase is accelerated relative to that observed for RQrev3B; in a similar manner, we observe an acceleration of this phase in the AA+3A reaction centers when compared to the AA and AA+4A reaction centers. If the acceleration of the slow phase of proton uptake in the RQrev3 reaction center reflected a change in an electron-transfer process, it would arise from a significant increase in the driving force for electron transfer in that reaction center compared to that of the RQrev3B strain. The similarity between the k_{AP} values measured in the two strains does not support any important increase in the free energy level of Q_A^- in the RQrev3 reaction center compared to that of the RQrev3B strain. The difference between the k_{BP} values measured in both strains (0.09 and $0.17\ s^{-1}$) reflects an increase of the driving force of less than 30 meV in the RQrev3 reaction center. According to Graige et al. *(47)*, if the process were electron-limited we should expect an acceleration of the process by <50%. This is far smaller than the >6-fold acceleration that we observe here (from 120 ms to ≤20 ms). [A similar conclusion can be drawn when the k_{BP} values are compared for newly constructed strains that carry only the M246Glu or M246Glu-M247Tyr mutations in the Q_A site (D. K. Hanson and P. Sebban, unpublished observations). At pH 7.5, the k_{BP} values for these reaction centers are $0.5\ s^{-1}$ and $0.3\ s^{-1}$, respectively (data not shown), which correspond to changes in the driving force of only ~20 meV between the two strains.] For the above reasons, the differences in the proton uptake kinetics measured in the reaction centers of the RQrev3 versus RQrev3B strains, and between those of the AA+3A versus the AA or AA+4A strains, reflect changes in the rates of proton transfer within the protein.

Role of Q_A-Site Mutations in Acceleration of Proton Transfer to Q_B. These results demonstrate the ability of the M247Tyr (or possibly the coupled M246Ala → Glu and M247Ala → Tyr) mutations to increase the rate of proton transfer to Q_B. The simplest interpretation of these data is that the Tyr substitution at M247 is responsible for the observed effects. However, with the current set of mutants, we cannot rule out the possibility that the effects we measure are due to a synergistic interaction of M246Glu and M247Tyr. Since these mutations are situated very near Q_A (Figure 1) and do not influence the electrostatic potential experienced by Q_B (Table 2), they may accelerate the partial protonation reactions near Q_B by opening up additional pathways for proton delivery to Q_B. Those pathways must extend to the region of the reaction center that is near the Q_A site. This possibility is supported by the measurements of proton uptake on the second flash. The substantial decrease in both the amplitude and lifetime of the slow phase of proton uptake in the AA+3A strain and its disappearance in the RQrev3 strain suggest that the Q_A^-site mutation(s) increase the number of groups that are able to deliver protons to Q_B on a rapid time scale. In these reaction centers, the

mutation(s) may increase the proton concentration near Q_A, perhaps by changing the properties of a large web of structured water molecules and strongly interacting ionizable groups *(6, 12*−*15*). In the high-resolution structures of the reaction centers of *Rb. sphaeroides* and *Rps. viridis*, several water molecules are located in a cavity at the interface of the H and M subunits with a minimal separation of 5.2 Å from Q_A *(14, 15*). It has been suggested that the Q_A water chain could be involved in proton uptake *(15*) and we propose that it can facilitate proton transfer to Q_B. The alanines at M246 and M247 are in the middle of a short α-helix; assuming no major rearrangement of the site, the side chain of M247Ala (M249 in *Rb. sphaeroides*) points away from Q_A toward the water-filled cavity in the structure of the *Rb. sphaeroides* reaction center *(3, 4, 6*). The substitution of the alanines at M246 and M247 by the larger Glu and Tyr, respectively, would require a slight movement of the polypeptide backbone, allowing reorientation of side chains to relieve crowding. When M247Ala is replaced by Tyr, its hydroxyl oxygen could exclude two of the water molecules in the cavity "under" Q_A. In this way, M247Tyr could connect to the network of water molecules that is present in the wild-type structure, helping to delocalize protons to the environment of Q_B.

ACKNOWLEDGMENT

We thank Dr. L. Baciou for very helpful discussions during this work and for critical reading of the manuscript, Dr. Raj Pokkuluri for the structure figure, and the editor for assistance above and beyond the call of duty. M. C. Gonnet is acknowledged for technical assistance with the reaction center preparations.

REFERENCES

1. Deisenhofer, J., Epp, O., Sinning, I., and Michel, H. (1995) *J. Mol. Biol. 246*, 429−457.
2. Allen, J. P., Feher, G., Yeates, T. O., Komiya, H., and Rees, D. C. (1988) *Proc. Natl. Acad. Sci. U.S.A. 85*, 8487−8491.
3. Chang, C.-H., El-Kabbani, O., Tiede, D., Norris, J., and Schiffer, M. (1991) *Biochemistry 30*, 5352−5360.
4. Ermler, U., Fritzsch, G., Buchanan, S. K., and Michel, H. (1994) *Structure 2*, 925−936.
5. Arnoux, B., Gaucher, J. F., Ducruix, A., and Reiss, F. (1995) *Acta Crystallogr. D 51*, 368−379.
6. Stowell, M. H. B., McPhillips, T. M., Rees, D. C., Soltis, S. M., Abresch, E., and Feher, G. (1997) *Science 276*, 812−816.
7. McAuley-Hecht, K. E., Fyfe, P. K., Ridge, J. P., Prince, S. M., Hunter, C. N., Isaacs, N. W., Cogdell, R. J., and Jones, M. R. (1998) *Biochemistry 37*, 4740−4750.
8. Leibl, W., and Breton, J. (1991) *Biochemistry 30*, 9634−9642.
9. Tiede, D. M., Vazquez, J., Cordova, J., and Marone, P. (1997) *Biochemistry 35*, 10763−10775.
10. Li, J., Gilroy, D., Tiede, D. M., and Gunner, M. R. (1998) *Biochemistry 37*, 2818−2829.
11. Beroza, P., Fredkin, D. R., Okamura, M. Y., and Feher, G. (1992) In *The Photosynthetic Reaction Center II* (Breton, J., and Verméglio, A., Eds.) pp 363−374, Plenum Press, New York.
12. Beroza, P., Fredkin, D. R., Okamura, M. Y., and Feher, G. (1995) *Biophys. J. 68*, 2233−2250.
13. Sebban, P., Maróti, P., Schiffer, M., and Hanson, D. K. (1995) *Biochemistry 34*, 8390−8397.
14. Lancaster, C. R. D., Michel, H., Honig, B., and Gunner, M. R. (1996) *Biophys. J. 70*, 2469−2492.
15. Fritzsch, G., Ermler, U., and Michel, H. (1995) in *Photosynthesis: from Light to Biosphere* (Mathis, P., Ed.) Vol. I, pp 599−602, Kluwer, Dordrecht, The Netherlands.
16. Hanson, D. K., Baciou, L., Tiede, D. M., Nance, S. L., Schiffer, M., and Sebban, P. (1992) *Biochim. Biophys. Acta 1102*, 260−265.
17. Hanson, D. K., Tiede, D. M., Nance, S. L., Chang, C.-H., and Schiffer, M. (1993) *Proc. Natl. Acad. Sci. U.S.A. 90*, 8929−8933.
18. Baciou, L., and Michel, H. (1995) *Biochemistry 34*, 7967−7972.
19. Takahashi, E., and Wraight, C. A (1996) *Proc. Natl. Acad. Sci. U.S.A. 93*, 2640−2645.
20. Miksovska, J., Valerio-Lepiniec, M., Schiffer, M., Hanson, D. K., and Sebban, P. (1998) *Biochemistry 37*, 2077−2083.
21. Takahashi, E., and Wraight, C. A. (1990) *Biochim. Biophys. Acta 1020*, 107−111.
22. Paddock, M. L., Rongey, S. H., McPherson, P. H., Juth, A., Feher, G., and Okamura, M. Y. (1994) *Biochemistry 33*, 734−745.
23. Paddock, M. L., Rongey, S. H., Feher, G., and Okamura, M. Y. (1989) *Proc. Natl. Acad. Sci. U.S.A. 86*, 6602−6606.
24. Takahashi, E., and Wraight, C. A. (1992) *Biochemistry 31*, 855−866.
25. Shinkarev, V. P., Takahashi, E., and Wraight, C. A. (1993) *Biochim. Biophys. Acta 1142*, 214−216.
26. McPherson, P. H., Schoenfeld, M., Paddock, M. L., Okamura, M. Y., and Feher, G. (1994) *Biochemistry 33*, 1181−1193.
27. Miksovska, J., Kálmán, L., Schiffer, M., Maróti, P., Sebban, P., and Hanson, D. K. (1997) *Biochemistry 36*, 12216−12226.
28. Hanson, D. K., and Schiffer, M. (1998) *Photosynth. Res. 55*, 275−280.
29. Maróti, P., Hanson, D. K., Baciou, L., Schiffer, M., and Sebban, P. (1994) *Proc. Natl. Acad. Sci. U.S.A. 91*, 5617−5621.
30. Schiffer, M., Chan, C.-K., Chang, C.-H., DiMagno, T. J., Fleming, G. R., Nance, S., Norris, J., Snyder, S., Thurnauer, M., Tiede, D. M., and Hanson, D. K. (1992) in *The Photosynthetic Reaction Center II* (Breton, J., and Verméglio, A., Eds.) pp 351−361, Plenum Press, New York.
31. Bylina, E. J., Ismail, S., and Youvan, D. C. (1986) *Plasmid 16*, 175−181.
32. Bylina, E. J., Jovine, R. V. M., and Youvan, D. C. (1989) *Biotechnology 7*, 69−74.
33. Baciou, L., Bylina, E. J., and Sebban, P. (1993) *Biophys. J. 65*, 652−660.
34. Paddock, M. L., Feher, G., and Okamura, M. Y. (1991) *Photosynth. Res. 27*, 109−119.
35. Verméglio, A. (1977) *Biochim. Biophys. Acta 459*, 516−524.
36. Wraight, C. A. (1977) *Biochim. Biophys. Acta 459*, 525−531.
37. Wraight, C. A. (1981) *Isr. J. Chem. 21*, 348−354.
38. Valerio-Lepiniec, M., Delcroix, J.-D., Schiffer, M., Hanson, D. K., and Sebban, P. (1997) *FEBS Lett. 407*, 159−163.
39. McPherson, P. H., Okamura, M. Y., and Feher, G. (1988) *Biochim. Biophys. Acta 934*, 348−368.
40. Maróti, P., and Wraight, C. A. (1988) *Biochim. Biophys. Acta 934*, 329−347.
41. Takahashi, E., Maróti, P., and Wraight, C. A. (1992) in *Electron and Proton Transfer in Chemistry and Biology* (Müller, A., Ratajczak, H., Junge, W., and Diemann, E., Eds.) pp 219−236, Elsevier, Amsterdam.
42. Rongey, S. H., Paddock, M. L., Feher, G., and Okamura, M. Y. (1993) *Proc. Natl. Acad. Sci. U.S.A. 90*, 1325−1329.
43. Brzezinski, P., Paddock, M. L., Okamura, M. Y., and Feher, G. (1997) *Biochim. Biophys. Acta 1391*, 146−156.
44. Nabedryk, E., Breton, J., Hienerwadel, R., Fogel, C., Mantele, W., Paddock, M. L., and Okamura, M. L. (1995) *Biochemistry 34*, 14722−14732.
45. . Alexov, E., and Gunner, M. R. (1997) *Biophys. J. 72*, 2075−2093.
46. Graige, M. S., Paddock, M. L., Feher, G., and Okamura, M. Y. (1996) *Biophys. J. 70*, 11.
47. Graige, M. S., Paddock, M. L., Bruce, J. M., Feher, G., and Okamura, M. Y. (1996) *J. Am. Chem. Soc. 118*, 9005−9016.

BI980500T